Rare Metal Materials and Engineering
Volume 54, Issue 2, February 2025
Available online at www.rmme.ac.cn

Science Press

Cite this article as: Zhang Wenxin, Zhang Xiankun, Shi Lei, et al. Dissimilar Friction Stir Lap Welding of Ti Alloy and Al-Li Alloy: Microstructure and Mechanical Property[J]. Rare Metal Materials and Engineering, 2025, 54(02): 311-318. https://doi.org/10.12442/j.issn.1002-185X.20240605.

ARTICLE

Dissimilar Friction Stir Lap Welding of Ti Alloy and Al-Li Alloy: Microstructure and Mechanical Property

Zhang Wenxin[1,2], Zhang Xiankun[1,2], Shi Lei[1,2], Li Shengli[1,2], Jiang Yuanning[1,2], Wu Chuansong[1,2]

[1] State Key Laboratory of Advanced Equipment and Technology for Metal Forming, Shandong University, Jinan 250061, China; [2] Key Laboratory for Liquid-Solid Structure Evolution & Processing of Materials, Ministry of Education, Shandong University, Jinan 250061, China

Abstract: Friction stir lap welding of AA2195 Al-Li alloy and Ti alloy was conducted to investigate the formation, microstructure, and mechanical properties of the joints. Results show that under different welding parameters, with the decrease in welding heat input, the weld surface is smoother. The Ti/Al joint interface is flat without obvious Ti and Al mixed structure, and the hook structure is not formed under optimal parameters. Due to the enhanced breaking effect of the stirring head, the hook structural defects and intermetallic compounds are more likely to form at the Ti/Al interface at high rotational speed of 1000 r/min, thereby deteriorating the mechanical properties of joints. Decreasing the heat input is beneficial to hardness enhancement of the aluminum alloy in the weld nugget zone. Under the optimal parameters of rotation speed of 800 r/min and welding speed of 120 mm/min, the maximum tensile shear strength of joint is 289 N/mm.

Key words: Ti/Al dissimilar welding; friction stir lap welding; Ti alloy; Al-Li alloy; interface bonding; mechanical property

Al-Li alloy has high specific strength and stiffness, good corrosion resistance, and excellent low-temperature fatigue performance, which has a wide application prospect in the aerospace field[1–3]. Ti alloy has excellent mechanical properties, particularly high-temperature performance and good corrosion resistance, so it is commonly used in industrial fields[4–5]. However, huge differences exist in the physical and chemical properties between Al-Li and Ti alloys, such as melting point, thermal conductivity, and linear expansion coefficient[6]. In addition, Al, Li, and Ti elements are active and easy to react with oxygen in the air, therefore producing oxides which are easy to mix in the joint and affect the joint performance[7]. Besides, intermetallic compounds (IMCs), such as $TiAl_3$, can be formed between Al and Ti. Excessively thick IMCs will deteriorate the mechanical properties of the joints, inhibiting the formation of ideal Ti/Al hybrid structure[8–9].

Currently, the welding methods for Al/Ti dissimilar metal joints can be categorized as fusion welding, brazing, fusion brazing, and solid-state welding. The fusion welding of Al/Ti dissimilar materials will produce unacceptable defects, such as large distortion and residual stress, pores, grain coarsening, and the formation of a large number of IMCs at the interface[10–11]. As a traditional welding method for dissimilar metals, the application of brazing is restricted by its low welding efficiency and high cost due to the equipment conditions and workpiece size[12–13]. As a type of solid-state welding technique, friction stir welding (FSW) has the advantages of low temperature, low energy consumption, no splash, and no smoke[14–16]. No melting or solidification process exists in FSW procedure, which can avoid the defect formation, and the interface behavior of Al and Ti is easier to control[17–19].

Geyer et al[20] studied the interface stress distribution and microstructure of the joint after friction stir lap welding of Al/Ti dissimilar metals. The tip shape and length of FSW tool varied in the research, and it is found that a good joint can be obtained by a short FSW tool with hemispherical tip. Yazdanian et al[21] studied the effect of pin size and interlayer on the interface bonding and fatigue strength of

Received date: September 18, 2024
Foundation item: National Natural Science Foundation of China (52275349); Key Research and Development Program of Shandong Province (2021ZLGX01)
Corresponding author: Shi Lei, Ph. D., Professor, State Key Laboratory of Advanced Equipment and Technology for Metal Forming, Shandong University, Jinan 250061, P. R. China, Tel: 0086-531-88395987, E-mail: lei.shi@sdu.edu.cn

FSWed AA2024-Ti6Al4V lap joints. It is found that the high fatigue strength of the weld is not sensitive to parameter variation, such as the stirring head size. At present, the research on the connection between Ti and Al-Li alloys is rarely reported. Using Al-Li alloy instead of traditional Al alloy can reduce the mass of structural parts by more than 15% and simultaneously increase the stiffness by 10%–20%, showing great potential as the ideal lightweight structural materials. Al-Li alloys exhibit lower melting point, smaller density, and higher thermal conductivity, leading to greater disparity in physical and chemical properties between Al-Li alloys and Ti alloys. Therefore, the difficulty of FSW process of Al-Li and Ti alloys will be greater than that of ordinary Al alloy[22–23].

In this research, the friction stir lap welding was conducted on AA2195 Al-Li alloy and Ti alloy. The joint formation, microstructure, and mechanical properties of the weld were investigated.

1 Experiment

In this research, AA2195 Al-Li alloy and TC4 Ti alloy were used as base metals (BMs). The AA2195 Al-Li alloy was pre-processed by artificial aging treatment after solid solution (T6). Table 1 shows the chemical composition of AA2195 Al-Li and TC4 Ti alloys. The tensile shear strength of AA2195 Al-Li alloy is 540.8 MPa and its elongation is 21.2%. The tensile shear strength of TC4 Ti alloy is 895 MPa and its elongation is 10%. The size of Al plate and Ti plate was 200 mm× 50 mm×2 mm.

Fig. 1 shows the schematic diagram of friction stir lap welding used in this research. Heat-affected zone (HAZ), stir zone (SZ), and thermo-mechanically affected zone (TMAZ) can be observed. During the welding process, the Al-Li alloy plate was on the upper side and placed on the retreating side (RS), and the Ti alloy plate was at the lower side and placed on the advancing side (AS). The lap width was 25 mm, and the weld was positioned at the center of lap area. BMs were polished before welding to remove the surface oxide film. Firstly, three groups of experiment parameters were set: (1) rotation speed of 800 r/min with welding speed of 60 mm/min, namely 800-60 condition; (2) rotation speed of 800 r/min with welding speed of 120 mm/min, namely 800-120 condition; (3) rotation speed of 800 r/min with welding speed of 240 mm/min, namely 800-240 condition. After experiments, cracking phenomenon occurred at the interface of the sample under 800-240 condition. Therefore, the 800-240 condition was adjusted to rotation speed of 1000 r/min with welding speed of 240 mm/min, namely 1000-240 condition. During the welding process, the inclination angle of friction stir lap welding tool was set as 2.5° , and the plunged depth of the shoulder was 0.2 mm. The material of friction stir lap welding tool was WRe alloy, and the shoulder diameter was 12 mm. The friction stir lap welding tool was conical and had a right-handed thread on the surface, and it rotated counterclockwise during operation. The diameter of the stirring head tip was 3 mm, the diameter of the stirring head root was 4 mm, and the length of stirring head was 2.1 mm.

Table 1 Chemical composition of AA2195 Al-Li and TC4 Ti alloys (wt%)[22,24]

Alloy	Cu	Li	V	Fe	Mg	Al	Ti
AA2195-T6	4.01	1.02	-	≤0.15	0.52	Bal.	≤0.15
TC4	-	-	4.00	0.026	-	6.00	Bal.

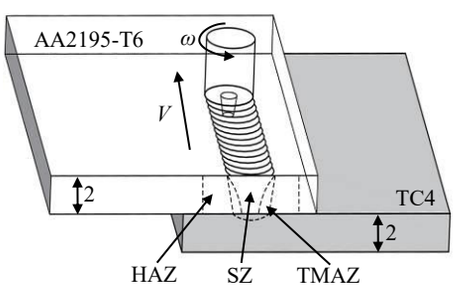

Fig.1 Schematic diagram of friction stir lap welding process of Al-Li/Ti alloys

Optical microscope (OM), field emission scanning electron microscope (SEM), and energy dispersive X-ray spectrometer (EDS) were used to observe and analyze the microstructure of the joint. As shown in Fig. 2, the test sample was cut perpendicularly to the welding direction by wire electrical discharge machining (WEDM) to obtain OM sample of 20 mm×8 mm in size. Subsequently, the sample was polished by 200# – 1200# sandpaper and then polished by diamond polishing agent (0.5 μm). Keller reagent (2.5 mL HNO_3+1.5 mL HCl+1 mL HF+95 mL H_2O) was applied for 45 s to etch OM samples after polishing. Zeiss Smartzoom5 microscope was used to observe the macroscopic morphology, and LV 150 N metallographic microscope was used to observe the joint microstructure. The interface microstructure was characterized by SEM and EDS to further analyze the distribution and types of elements.

Before tensile tests, WEDM residual trace was removed by sandpaper grinding to avoid stress concentration. The tensile test was conducted by WDW-100AE universal electronic tensile testing machine, and the loading rate was 1 mm/min. During the test, a compensation piece with size of 20 mm×15 mm×2 mm was pasted on the back of Al and Ti plates on both

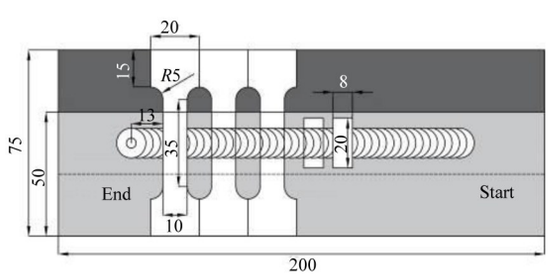

Fig.2 Schematic diagram of cutting position

sides to reduce the torque generated during the tension-shear process.

HVS-1000Z-W automatic turret Vickers microhardness tester was used to test the microhardness of the welded joint section parallel or perpendicular to the interface, as shown in Fig. 3. When the section was parallel to the interface, the distance between the test point and the upper/lower surface of the Al-Li alloy plate was 1 mm, and the test spacing was 0.5 mm. When the section was perpendicular to the interface, the test point was located at the horizontal center of the weld, and the test spacing was 0.25 mm. The test load was 2.94 N and the dwelling time was 10 s.

2 Results and Discussion

2.1 Surface forming

Fig. 4 shows the surface morphologies of Al-Li/Ti friction stir lap welded joints under different process parameters. Under the 800-60 condition, the weld surfaces present good forming effect without groove defects, but a small amount of flash is formed on both sides of the weld. When the welding speed reaches 120 mm/min, the weld surface becomes smoother without visible flash. This is because the friction heat is decreased with the increase in welding speed, leading to the reduction in the amount of flash.

Eq.(1) presents the formula of heat input[25], as follows:

$$T/T_m = K\left[\omega^2/(2.362v \times 10^4)\right]^{\alpha} \quad (1)$$

where ω is the rotational speed, v is the welding speed, α is the exponent ranging from 0.04 to 0.06, K is a constant between 0.65 and 0.75, and T_m (℃) represents the melting point of the alloy. When the rotation speed increases to 1000 r/min and the welding speed also increases to 240 mm/min, the heat input in friction stir lap welding process is directly proportional to ω^2/v, according to Eq. (1). The heat input is minimized when the welding parameters are set as rotation speed of 1000 r/min and welding speed of 240 mm/min, resulting in the smoothest weld surface in this research.

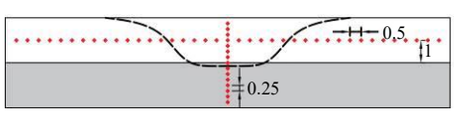

Fig.3 Distributions of microhardness test points on cross-section of welded joint

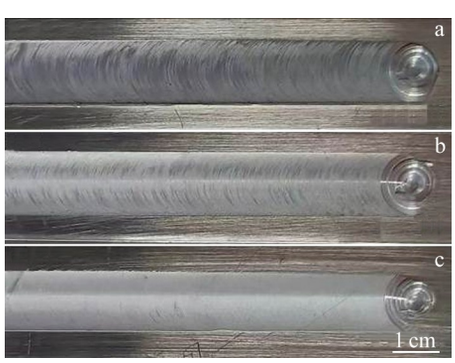

Fig.4 Surface morphologies of Al-Li/Ti friction stir lap welded joints under 800-60 condition (a), 800-120 condition (b), and 1000-240 condition (c)

2.2 Macromorphology of weld cross-section

Fig. 5 shows the cross-section morphologies of Al-Li/Ti friction stir lap welded joints under different conditions. No hook structure is formed and no obvious Ti particles are mixed in the Al alloy. It is speculated that because the welding heat input is too low and Ti alloy has high strength during friction stir lap welding, which result in difficulty for deformation under the mechanical action of friction stir lap welding tool, obvious Al-Ti particle mixed structure and hook structure can hardly be formed. Another possible reason is that the length of the friction stir lap welding tool is 2.1 mm and the plunge depth of shoulder is 0.2 mm, so the friction stir lap welding tool cannot penetrate the high-strength Ti alloy plate, thereby barely forming Al-Ti particle mixed structure and hook structure.

2.3 Microstructure

According to the locations in the weld and microstructure, the welded joints can be divided into BM, HAZ, TMAZ, SZ, and interface (Fig. 5a). Under the 800-120 condition, OM microstructures of different regions of the Al-Li/Ti friction stir lap welded joint are observed, as shown in Fig. 6. It can be seen that the grain structure of Al-Li alloy in HAZ is composed of coarse lath grains. This is because the Al-Li alloy is affected by the welding heat during the welding process, resulting in the growth of grains. The microstructure of TMAZ is composed of elongated deformed grains and fine equiaxed grains. This is because TMAZ is close to the friction stir lap welding tool, which is subject to higher temperature thermal cycle, and a certain plastic deformation occurs. Therefore, TMAZ undergoes incomplete dynamic recrystallization, as shown in Fig. 6a. SZ is directly affected by the friction stir lap welding tool. Under the action of plastic deformation and high temperature, complete dynamic recrystallization occurs. Because of different rotation directions of the friction stir

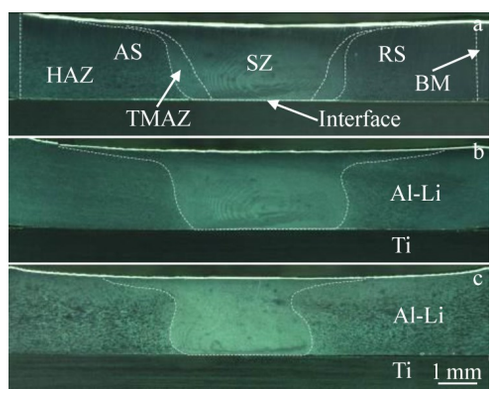

Fig.5 Cross-section morphologies of Al-Li/Ti friction stir lap welded joints under 800-60 condition (a), 800-120 condition (b), and 1000-240 condition (c)

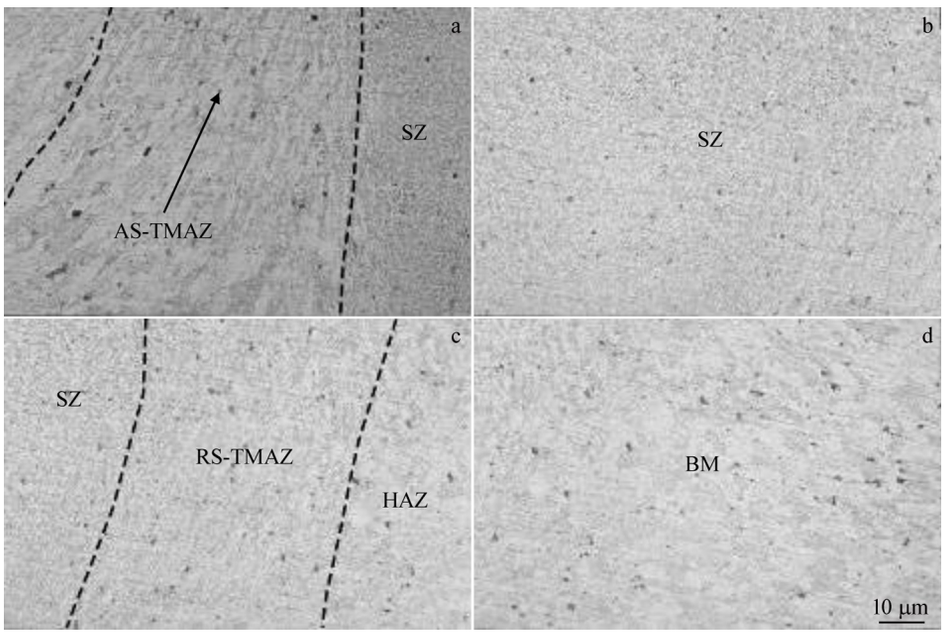

Fig.6 OM microstructures of different regions of Al-Li/Ti friction stir lap welded joint under 800-120 condition: (a) AS-TMAZ, (b) SZ, (c) RS-TMAZ-HAZ, and (d) BM

lap welding tool, AS and RS of TMAZ undergo different deformation processes, resulting in different microstructures. The grains of BM are finer than those of HAZ, because they are less affected by heat.

2.4 IMCs

Fig. 7 and Fig. 8 show SEM images of the interfaces of Al-Li/Ti friction stir lap welded joint under 800-60 condition and 800-120 condition, respectively. It can be seen that the weld interface is relatively flat without hook structure. Boundaries exist between connected and unconnected areas on AS and RS. No clear Ti alloy particles exist in the Al-Li alloy. Fig. 9 shows EDS line scanning results of the marked lines in Fig. 7c and Fig. 8c. According to the analysis results, no IMCs are produced.

Fig. 10 shows SEM images of the interface of Al-Li/Ti friction stir lap welded joint under 1000-240 condition. The small hook defects can be observed on AS of interface and the Ti particles are mixed within the Al-Li alloy. According to the element distributions of interface of Al-Li/Ti friction stir lap welded joint (Fig. 10h – 10i), it can be found that a horizontal section appears on the broken line, indicating that elements are diffused mutually to form a diffusion layer

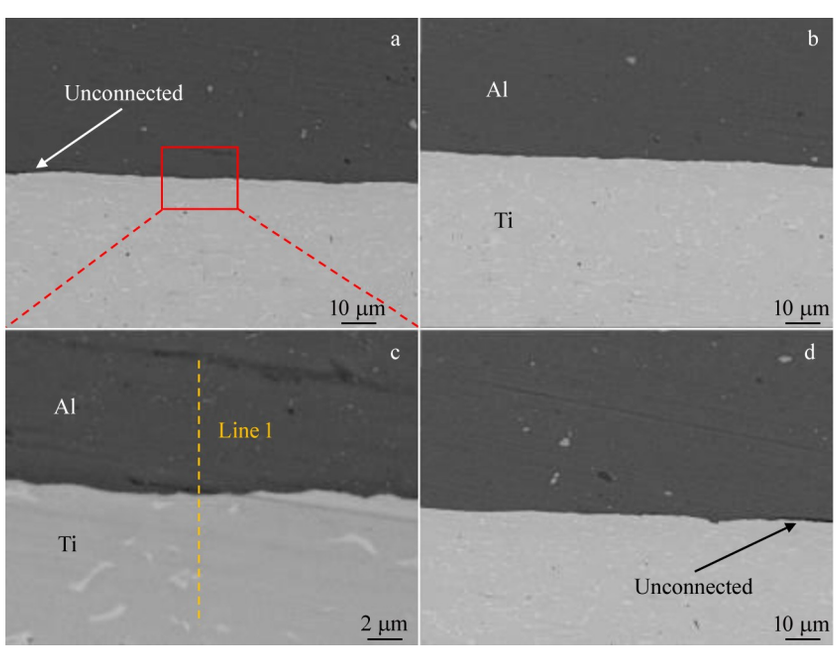

Fig.7 SEM images of different regions of Al-Li/Ti friction stir lap welded joints under 800-60 condition: (a, c) AS, (b) SZ, and (d) RS

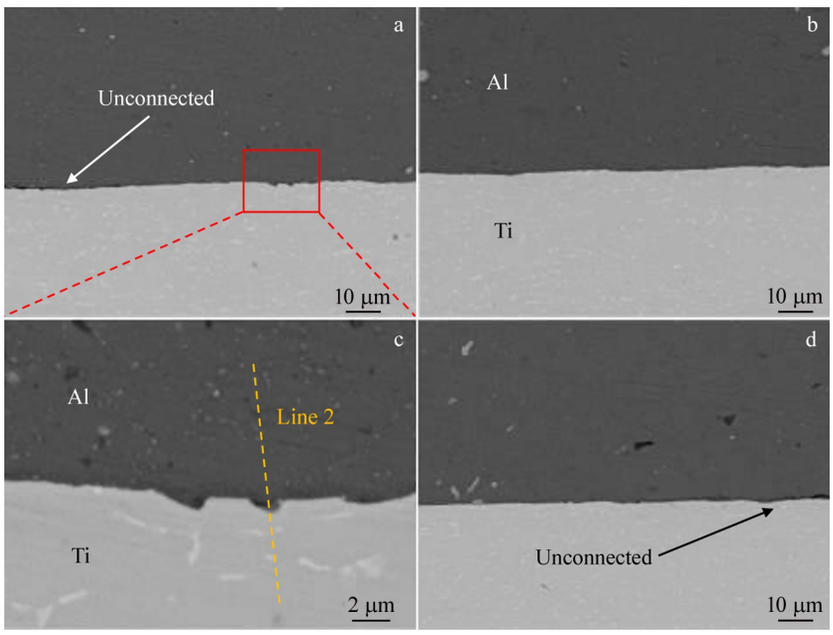

Fig.8 SEM images of different regions of Al-Li/Ti friction stir lap welded joints under 800-120 condition: (a, c) AS, (b) SZ, and (d) RS

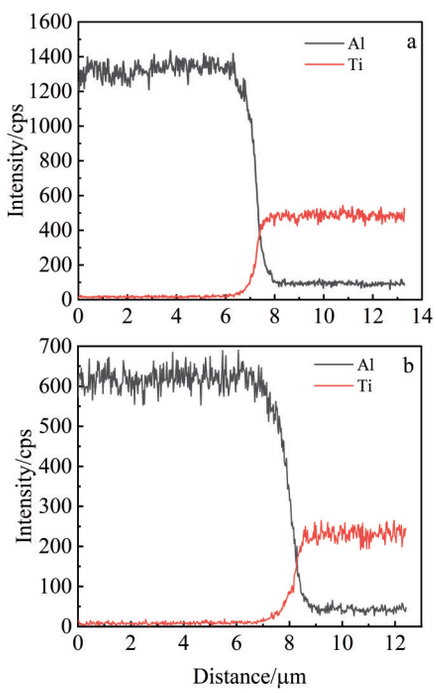

Fig.9 EDS line scanning results of line 1 in Fig.7c (a) and line 2 in Fig.8c (b)

rich in Al and Ti elements. Because increasing the rotational speed promotes the breaking effect of friction stir lap welding tool on Ti alloy, forming hook-like structures and IMCs. The maximum thickness of IMC is approximately 0.56 μm, as shown in Fig.10f. The composition of IMCs is detected, and the results are shown in Table 2. It can be seen that there are mainly two IMCs: $TiAl_3$ and TiAl. Cracking can also be observed at the interface joint on RS, which may impact the mechanical properties of the joint.

2.5 Mechanical properties

2.5.1 Microhardness

The microhardness distributions of the Al-Li/Ti friction stir lap welded joint under different conditions are shown in Fig.11. It can be seen that the transverse microhardness of the Al-Li alloy structure presents inverted V-type distribution. This is because HAZ is too large, but the sample length is short. Therefore, the test point does not quite locate at BM, resulting in the fact that the sample microhardness is lower than BM microhardness. The minimum microhardness occurs at the sample boundary, and it increases as the test point moves towards SZ. The microhardness of the joint under 1000-240 condition is higher than that under 800-120 and 800-60 conditions. Because of higher welding heat input, the recrystallized grains are easy to grow after welding, which degrades the microhardness of the weld[26]. The longitudinal microhardness of the Ti alloy side of the weld has a fluctuation to some extent. Overall, the microhardness of the weld nugget zone increases. The uniformity of Al-Li alloy side does not have obvious change.

2.5.2 Shear strength

Fig. 12 shows the comparison of mechanical properties of Al-Li/Ti friction stir lap welded joints under different conditions. When the welding speed is 60 mm/min, the tensile shear strength of the joint is 270 N/mm. However, when the welding speed increases to 120 mm/min, the tensile shear strength of the joint rises to 289 N/mm.

It is theorized that with the increase in welding speed, the welding heat input is decreased, leading to the reduction in the Al-Li/Ti mixed structure near the interface, which also alleviates the post-welding stress of interface and thereby enhances the shear strength of joint. Under the 800-120

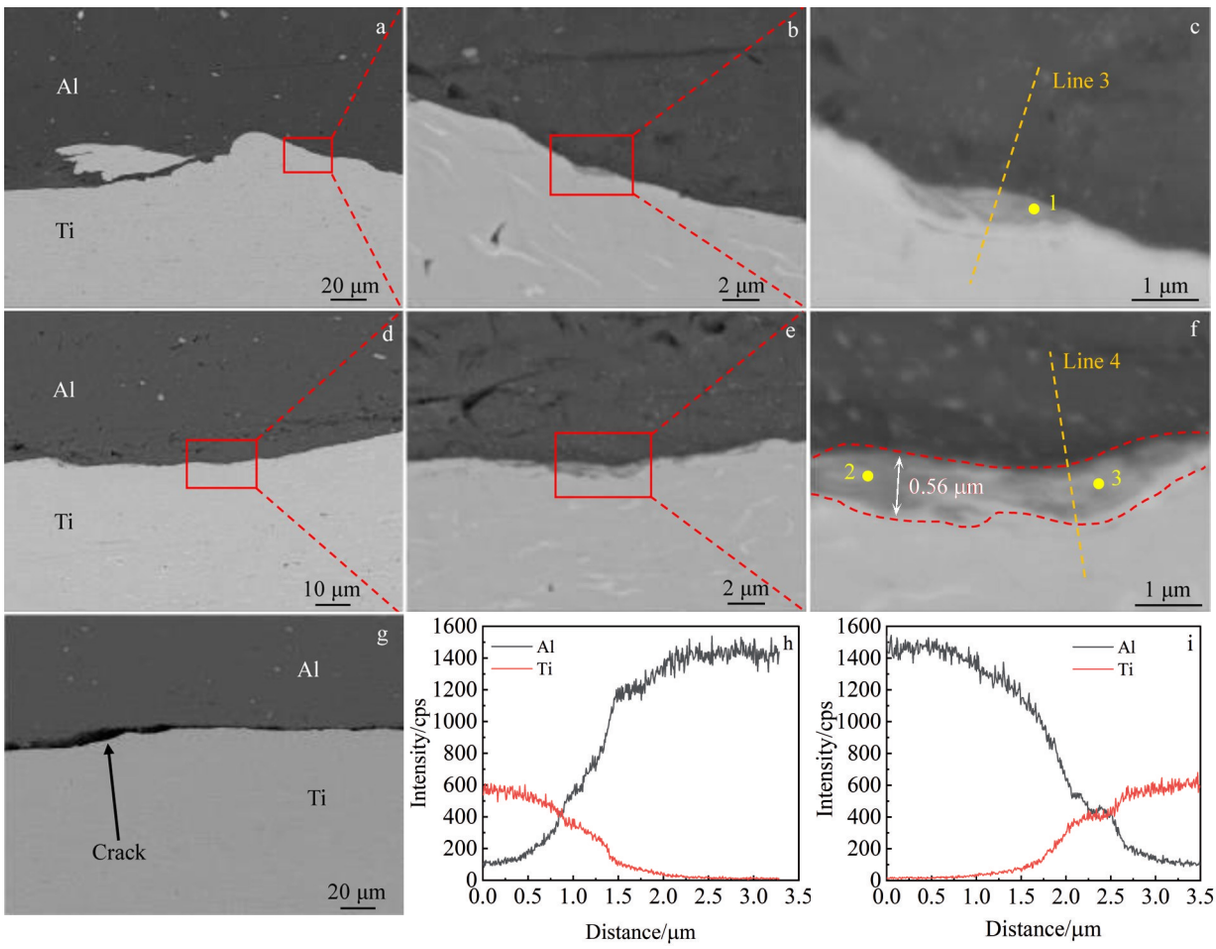

Fig.10 SEM images of AS (a–c), SZ (d–f), and RS (g) regions of Al-Li/Ti friction stir lap welded joints under 1000-240 condition; EDS line scanning results of line 3 in Fig.10c (h) and line 4 in Fig.10f (i)

Table 2 EDS point scanning results of Fig.10 (at%)

Point	Ti	Al	Possible IMC phase
1	27.3	72.7	$TiAl_3$
2	50.8	49.2	TiAl
3	51.5	48.5	TiAl

condition, the maximum tensile shear strength of 289 N/mm can be achieved, which increases by 15%, compared with that with hook-like structures. When the rotation speed increases from 800 r/min to 1000 r/min and the welding speed increases to 240 mm/min, the tensile shear strength of the joint decreases from 289 N/mm to 259 N/mm due to cracks on RS side of joint, as shown in Fig.10g, leading to the reduction in the tensile shear strength of joint. Briefly, 800-120 condition is the optimal condition for Al-Li/Ti friction stir lap welded joint, which can achieve optimal microstructure and mechanical properties.

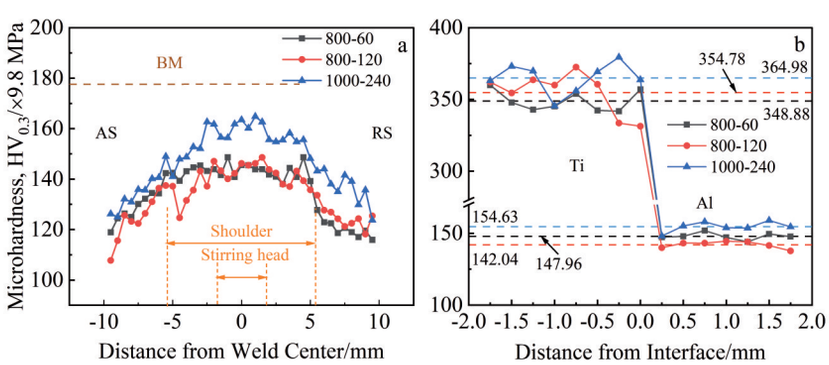

Fig.11 Microhardness distributions of Al-Li/Ti friction stir lap welded joints under different conditions: (a) parallel to interface; (b) along weld centerline

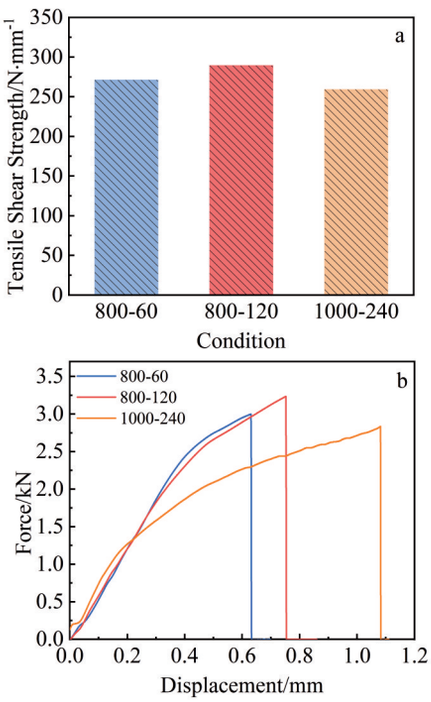

Fig.12 Tensile shear properties of Al-Li/Ti friction stir lap welded joints under different conditions: (a) tensile shear strength and (b) force-displacement curves

3 Conclusions

1) Al-Li/Ti friction stir lap welded joints without hook structural defects can be obtained under optimal welding conditions of rotation speed of 800 r/min and welding speed of 120 mm/min, whose tensile shear strength is 289 N/mm, increased by 15%, compared with that of joints with hook-like structures.

2) Decreasing the heat input during welding process results in the smoother surface for Al-Li alloy and the gradual decrease in flash defects. Furthermore, the microhardness of the weld nugget zone increases.

3) Under optimal parameters, no significant IMCs can be observed at the interface of Al-Li/Ti friction stir lap welded joint. However, increasing the rotation speed promotes the breaking effect of the friction stir lap welding tool on Ti alloy, leading to the formation of hook-like structures and IMCs, which deteriorates the mechanical performance of joints.

References

1 Xiao G Z, An R Yang J X *et al*. *Advanced Engineering Materials*[J], 2024, 26(12): 2301639

2 Wu J L, Li L, Dai L *et al*. *Journal of Alloys and Compounds*[J], 2024, 1004: 175841

3 Chen P, Wang J, Liu G *et al*. *Materials Science and Engineering A*[J], 2024, 914: 147165

4 Yan T Y, Liu Y, Wang J F *et al*. *Journal of Materials Science & Technology*[J], 2024, 174: 1

5 Li Z, Zhao W, Yu K D *et al*. *Journal of Rare Earths*[J], 2024, 42(3): 586

6 Gadakh V S, Badheka V J, Mulay A S. *Proceedings of the Institution of Mechanical Engineers Part L-Journal of Materials, Design and Applications*[J], 2021, 235(8): 1757

7 Wang S, Li Y, Yang Y *et al*. *Journal of Manufacturing Processes*[J], 2021, 70: 300

8 Liu S X, Chen F R, Fan Y F *et al*. *Rare Metal Materials and Engineering*[J], 2024, 53(7): 1863

9 Zuo Y Y, Liu H J, Li D R *et al*. *The International Journal of Advanced Manufacturing Technology*[J], 2024, 133(7–8): 3973

10 Zhou L, Yu M R, Zhao H Y *et al*. *Journal of Manufacturing Processes*[J], 2019, 48: 119

11 Wang Z W, Shen J Q, Hu S S *et al*. *Optics and Laser Technology* [J], 2022, 149: 107867

12 Evdokimov A, Doynov N, Ossenbrink R *et al*. *International Journal of Mechanical Sciences*[J], 2021, 190: 106019

13 Bang K S, Lee K J, Bang H S *et al*. *Materials Transactions*[J], 2011, 52(5): 974

14 Ahmed M M Z, El-Sayed Seleman M M, Fydrych D *et al*. *Materials*[J], 2023, 16(8): 2971

15 Muhammad N A, Geng P, Wu C *et al*. *International Journal of Machine Tools & Manufacture*[J], 2023, 186: 104004

16 Sun Jifeng, Ke Liming, Xu Yang *et al*. *Rare Metal Materials and Engineering*[J], 2023, 52(11): 3900 (in Chinese)

17 Zuo Y Y, Liu H J, Li D R *et al*. *Welding in the World*[J], 2024, 68: 2661

18 Saravana S A, Mugada K K, Kumar A. *Journal of Manufacturing Science and Engineering*[J], 2024, 146(2): 021004

19 Ugurlu M, Cakan A. *The International Journal of Advanced Manufacturing Technology*[J], 2023, 128(7–8): 3491

20 Geyer M, Avettand-Fenoel M N, Vidal V *et al*. *Journal of Manufacturing Processes*[J], 2024, 113: 360

21 Yazdanian S, Ales S, Chen Z W. *Welding in the World*[J], 2024, 68(8): 2217

22 Deng C M, Wang C M, Wang F F *et al*. *Materials Characterization*[J], 2022, 184: 111652

23 Sun S Y, Wang J, Gao B *et al*. *International Journal of Precision Engineering and Manufacturing*[J], 2024, 25(6): 1183

24 Zhang Zelong, Liu Qiang, Sun Chenyang *et al*. *Rare Metal Materials and Engineering*[J], 2023, 52(7): 2525 (in Chinese)

25 Mishra R S, Ma Z Y. *Materials Science and Engineering R: Reports*[J], 2005, 50(1–2): 1

26 Lyu X H, Tian C Y, Zhang W X *et al*. *Journal of Manufacturing Processes*[J], 2024, 124: 300

钛合金与铝锂合金异种搅拌摩擦搭接焊:组织与力学性能

张文鑫[1,2]，张贤昆[1,2]，石　磊[1,2]，李胜利[1,2]，蒋元宁[1,2]，武传松[1,2]
(1. 山东大学 金属成形高端装备与先进技术全国重点实验室，山东 济南 250061)
(2. 山东大学 材料液固结构演变与加工教育部重点实验室，山东 济南 250061)

摘　要：采用AA2195铝锂合金与钛合金进行搅拌摩擦搭接工艺试验，研究了焊缝成形、接头组织和力学性能。结果表明：在不同焊接参数条件下，随着焊接热输入的减小，焊缝表面更加光滑；Ti/Al接头界面平整，没有明显的Ti、Al混合，在最优参数下没有形成钩状结构。由于搅拌头的搅拌作用增强，在1000 r/min的高转速下，在Ti/Al界面处更容易形成钩状缺陷和金属间化合物，从而使接头的力学性能恶化。降低热输入有利于提高焊核区铝合金的硬度。在转速为800 r/min、焊接速度为120 mm/min的最优参数下，接头的最大抗剪强度为289 N/mm。

关键词：Ti/Al异种焊接；搅拌摩擦搭接焊；钛合金；铝锂合金；界面结合；力学性能

作者简介：张文鑫，男，2000年生，硕士生，山东大学金属成形高端装备与先进技术全国重点实验室，山东 济南 250061，电话：0531-88395987，E-mail：3176783390@qq.com